THE JOURNAL OF BIOLOGICAL CHEMISTRY VOL. 290, NO. 21, pp. 13064–13078, May 22, 2015


# Essential Role for Zinc Transporter 2 (ZnT2)-mediated Zinc Transport in Mammary Gland Development and Function during Lactation*

Received for publication, January 12, 2015, and in revised form, March 25, 2015 Published, JBC Papers in Press, April 7, 2015, DOI 10.1074/jbc.M115.637439

**Sooyeon Lee**[‡§¶], **Stephen R. Hennigar**[§], **Samina Alam**[¶‖], **Keigo Nishida****[‡‡], **and Shannon L. Kelleher**[‡§¶‖§§1]

*From the* [‡]*Interdisciplinary Graduate Physiology Program and* [§]*Department of Nutritional Sciences, The Pennsylvania State University, University Park, Pennsylvania 16802, Departments of* [¶]*Cellular and Molecular Physiology,* [§§]*Pharmacology, and* [‖]*Surgery, Penn State Hershey College of Medicine, Hershey, Pennsylvania 17033, **Laboratory for Homeostatic Network, RCAI, RIKEN Center for Integrative Medical Sciences (IMS-RCAI), Yokohama 230-0045, Japan, and* [‡‡]*Laboratory of Immune Regulation, Faculty of Pharmaceutical Sciences, Suzuka University of Medical Science, Suzuka 513-8670, Japan*

**Background:** ZnT2 is expressed in non-secreting and secreting mammary epithelium; however, the physiological role is not understood.
**Results:** ZnT2-null mice have impaired mammary expansion and compromised mammary differentiation and milk secretion during lactation.
**Conclusion:** ZnT2-mediated zinc transport is critical for mammary development and function during lactation.
**Significance:** This study identifies novel consequences of ZnT2 function in the mammary gland.

**The zinc transporter ZnT2 (*SLC30A2*) imports zinc into vesicles in secreting mammary epithelial cells (MECs) and is critical for zinc efflux into milk during lactation. Recent studies show that ZnT2 also imports zinc into mitochondria and is expressed in the non-lactating mammary gland and non-secreting MECs, highlighting the importance of ZnT2 in general mammary gland biology. In this study we used nulliparous and lactating ZnT2-null mice and characterized the consequences on mammary gland development, function during lactation, and milk composition. We found that ZnT2 was primarily expressed in MECs and to a limited extent in macrophages in the nulliparous mammary gland and loss of ZnT2 impaired mammary expansion during development. Secondly, we found that lactating ZnT2-null mice had substantial defects in mammary gland architecture and MEC function during secretion, including fewer, condensed and disorganized alveoli, impaired Stat5 activation, and unpolarized MECs. Loss of ZnT2 led to reduced milk volume and milk containing less protein, fat, and lactose compared with wild-type littermates, implicating ZnT2 in the regulation of mammary differentiation and optimal milk production during lactation. Together, these results demonstrate that ZnT2-mediated zinc transport is critical for mammary gland function, suggesting that defects in ZnT2 not only reduce milk zinc concentration but may compromise breast health and increase the risk for lactation insufficiency in lactating women.**

The mammary gland undergoes unique developmental processes that are regulated by a combination of hormones and growth factors to induce the physiological changes that occur during the transition from a non-secreting proliferative tissue into a highly differentiated secretory organ during lactation. Once differentiated, the secretory epithelium must be maintained to ensure milk production and offspring survival. A multitude of complex regulatory molecules that are involved in these morphological changes, such as prolactin, estrogen, and progesterone, have been well studied (1, 2). However, there is little understanding of non-hormonal factors that regulate mammary gland development and function.

Zinc is an ion that is required by 10% of the eukaryotic proteome and plays a vital role in >300 cellular functions including proliferation, apoptosis, cell signaling, and differentiation. Zinc deficiency results in profound defects in both non-lactating (3, 4) and lactating mammary tissue (5). Zinc transport is regulated by a network of zinc transporters that are categorized into two distinct families. Members of the ZIP family (ZIP1–14) facilitate cellular zinc uptake into the cytoplasm from across the cell membrane or from within intracellular compartments (6). In contrast, members of the ZnT[2] family (ZnT1–10) transport zinc from the cytosol, either across the cell membrane or into intracellular compartments (7).

ZnT2 (*SLC30A2*) is expressed in highly specialized secretory tissues, such as the pancreas, prostate, placenta, ovary, and mammary gland (8). ZnT2 functions as a dimer to transport zinc from the cytoplasm into vesicles (9–11). The ability to increase ZnT2 expression and vesicularize zinc protects cells from zinc cytotoxicity (9, 12). Most information on the role and regulation of ZnT2 function comes from studies in the lactating mammary gland and secreting mammary epithelial cells (MECs). ZnT2 is transcriptionally up-regulated by zinc as well as the lactogenic hormones prolactin and glucocorticoids (12, 13). In addition, ZnT2 is post-translationally regulated by pro-

* This work was supported, in whole or in part, by National Institutes of Health Grant R01HD058614 (to S. L. K.). This work was also supported by the Penn State Hershey College of Medicine Department of Surgery.
[1] To whom correspondence should be addressed: 500 University Dr., Hershey, PA. Tel.: 717-531-1778; Fax: 717-531-0884; E-mail: slk39@psu.edu.

[2] The abbreviations used are: ZnT, zinc transporter; MEC, mammary epithelial cell; MMP, matrix metalloproteinase; LD, lactation day; BSI, band signal intensity; CM, conditioned medium; MT, metallothionein.

lactin, leading to N-terminal (Lys-4/Lys-6) ubiquitination, which retargets ZnT2 to secretory vesicles to facilitate zinc accumulation, traffics ZnT2-containing vesicles to the cell membrane for zinc efflux into milk, and then activates proteasomal degradation to abrogate zinc secretion (10, 14). ZnT2 function in the mammary gland is not limited to lactation as it is also detected in the non-lactating mammary gland and non-secreting MECs (13, 15). In addition, ZnT2 imports zinc into mitochondria, which constricts ATP generation and activates apoptosis (15). This implicates ZnT2-mediated zinc transport in a plethora of cellular processes in the mammary gland; however, these roles are not well understood. The importance in understanding ZnT2 function and regulation reflects the fact that 5 missense mutations in *SLC30A2* have been identified (H54R, G87R, W152R, S296L, R340C) that reduce milk zinc concentration by 50–90% in breastfeeding women, causing severe neonatal zinc deficiency (11, 16–18), which clinically presents as alopecia and dermatitis, impaired neuronal and behavioral development, impaired immune function, and increased morbidity and mortality (19, 20). Therefore, understanding the role of ZnT2 in mammary gland biology has major implications for both infant and maternal health.

To better understand the role of ZnT2-mediated zinc transport in mammary gland biology, we used ZnT2-null mice and characterized the consequences of loss of ZnT2 function in both the nulliparous and lactating mammary gland. Although ZnT2-null mice were not zinc-deficient, they exhibited profound morphological defects in the mammary gland and MEC, indicating impairments in mammary gland development, lactational differentiation, and severe dysregulation in secretion pathways. Consistent with observations made in the mammary gland, ZnT2-attenuated MECs failed to activate differentiation and had impaired secretion of milk components. Moreover, although ZnT2-null dams had reduced milk zinc levels, they also had profound alterations in milk composition, including reduced protein, fat, and lactose concentrations compromising offspring survival. Our studies underscore the importance of ZnT2 in mammary gland biology and suggest that women with genetic variation in ZnT2 may have critical defects in mammary gland function and milk composition and secretion.

## Experimental Procedures

*Generation of ZnT2-null Mice*—All animal protocols were approved by the Institutional Animal Care and Use Committee at the Pennsylvania State University, which is accredited by the American Association for the Accreditation of Laboratory Animal Care. Heterozygous ZnT2 transgenic mice were generated by Dr. Keigo Nishida (Suzuka University of Medical Sciences, Suzuka, Japan) with the following targeting strategy; a neomycin cassette (Neo) was inserted into the *SLC30A2* (ZnT2) gene at position exons 5 and 6. Male and female heterozygous mice were mated to generate wild-type (*wt*) and ZnT2-null (*ZnT2ko*) mice. Offspring were genotyped by isolating DNA from ear snips using the Extract-N-Amp Tissue PCR kit (Sigma) followed by PCR amplification with primers (primer 1 (P1), 5′-CATTGCCCGCTTACCCTGAG-3′; Primer 2 (P2), 5′-GACTGATGGAGGGCCAACCCCATTC-3′; primer 3 (P3), 5′-CAGCAGCCTCTGTTCCACATACACTTCAT-3′).

PCR products generated from the P1/P2 primer set (256 bp) for the *wt* allele and the P1/P3 primer set (176 bp) for the *ZnT2ko* allele were run on a 1% agarose gel containing 0.1% ethidium bromide and visualized using UV light. Mice were housed in polycarbonate ventilated cages and fed *ad libitum* on a standard commercial rodent diet (LabDiet, Quakertown, PA). They were maintained on a 12-h light/dark cycle under controlled temperature and humidity.

*Nulliparous and Lactating Mice Experiments*—To study the nulliparous mammary gland, we used post-pubertal mice at 10 weeks of age during the proestrus/estrus phase to control for the morphological and cellular changes seen in the mammary gland throughout the estrous cycle (21). To study lactating mammary gland, *wt* and *ZnT2ko* female mice were mated with a *wt* male (2:1 ratio) for 2 weeks and allowed to deliver naturally and nurse their litters up to lactation day (LD) 10. The number of offspring was counted, litter size was normalized to 6–7 pups/dam on LD2, and the number of dams still nursing a litter and their litter size at LD10 was recorded to calculate the percent of dams maintaining litters. Nulliparous and lactating mice were euthanized by $CO_2$ asphyxiation, and tissues were immediately excised and mounted on slides, fixed in 4% paraformaldehyde, frozen in isopentane, or stored at −80 °C until analysis.

*Histological Analysis*—For histological examination, mammary glands were fixed in 4% paraformaldehyde in phosphate-buffered saline overnight and embedded in paraffin, and sections (5 $\mu$m) were stained with hematoxylin and eosin (H&E) or Masson's trichrome as previously described (3). The adipocyte size in three 10× fields of view per section from 5 mice/genotype was measured, and data were expressed as adipocyte area ($\mu m^2$) ±S.D. A TACS-XL Basic In Situ Apoptosis (TUNEL) detection kit was used to identify apoptotic cells according to the manufacturer's instruction (Trevigen, Inc., Gaithersburg, MD). The number of cells stained positive for TUNEL in five 40× fields of view per section ($n = 3$ mice/genotype) was counted, and data were expressed as a mean apoptotic cell number ±S.D. The following antibodies were used for immunofluorescent staining: anti-ZnT2 (1 $\mu$g/ml; Ref. 15), anti-F4/80 (macrophage marker, 1:50; Santa Cruz Biotechnology, Inc., Dallas, TX), and anti-Ki-67 (proliferation marker, 1:300; Vector Laboratories, Burlingame, CA). Antibodies were visualized with Alexa Fluor® 488 or Alexa Fluor® 568 (Life Technologies, Carlsbad, CA) and counterstained with DAPI nuclear stain (Life Technologies). Stained sections were examined using the Leica DM IL LED microscope equipped with a digital Leica DFC425 camera (Leica Microsystems, Buffalo Grove, IL) or the Leica Inverted Confocal Microscope SP8 (Leica Microsystems). The number of cells stained positive for Ki-67 in three 10× fields of view per section ($n = 5$ mice/genotype) was counted, and data were expressed as a mean % Ki-67$^+$ cells ±S.D.

*Whole Mount Analysis*—Mammary glands were fixed in Carnoy's solution overnight and stained with carmine alum, as previously described (3). Stained whole mounts were examined using Olympus microscope (BX6), and 4× objective images were automatically stitched on cellSens Dimension software. To quantify ductal length (mm), the distance between the cen-

ter of the lymph node and the distal end of the longest duct was measured using Adobe Photoshop CS3. The ductal length was measured in mammary glands ($n = 5$ mice/genotype), and data were expressed as mean ductal length (mm) ±S.D. The number of lateral branch points was measured in mammary glands ($n = 5$ mice/genotype), and data were expressed as mean number of branch points ±S.D. The ratio of glandular tissue to stromal was calculated by the area of glands over the area of adipose stroma in whole mount images (n = 5 mice/genotype), and data were expressed as mean glandular over stromal ratio ±S.D.

*Zinpyr-1 Imaging*—Frozen mammary glands were sectioned (5 μm), stained with 20 μM Zinpyr-1 and 0.5 μM DAPI diluted in saline (147 mM NaCl, 4 mM KCl, 3 mM $CaCl_2$, 9 mM $MgCl_2$, 11 mM HEPES, 10 mM glucose, pH 7.4), and rinsed in saline. Slides were immediately imaged on the DeltaVision Elite Inverted Microscope (Olympus, Tokyo, Japan).

*Transmission Electron Microscopy*—Excised mammary glands were immediately harvested in Karnovsy's fixative (4% paraformaldehyde, 1 M sodium hydrozide, 25% glutaraldehyde, 0.2 M sodium cacodylate, pH 7.3) for 24 h and stored in 0.1 mM sodium cacodylate until processed and imaged with a JEOL JEM1400 Digital Capture transmission electron microscope at the Penn State Hershey College of Medicine Imaging Facility.

*Immunoblotting*—Tissue and cell lysates were prepared in homogenization buffer (20 mM HEPES, pH 7.4, 1 mM EDTA, 250 mM sucrose) containing protease inhibitors, and total cell lysate or membrane fractions were prepared as previously described (3). Proteins (20 μg) were prepared, electrophoresed, and immunoblotted as previously described (3, 10). The following antibodies were used: anti-ZnT2 (1 μg/ml); anti-MMP-2 (1:1000; Abcam, Cambridge, MA), anti-MMP-9 (1:1000; Abcam) anti-p-Stat5, and anti-Stat5 (1:1000; Cell Signaling, Danvers, MA), anti-p-Stat3 and anti-Stat3 (1:1000; Cell Signaling), anti-β-casein (1:1000; Santa Cruz Biotechnology, Inc.), and anti-β-actin (1:5000, Sigma). Antibodies were detected with IRDyes® (1:20,000; LI-COR Biosciences, Lincoln, NE). Proteins were scanned on the Odyssey® CLX imaging system (LI-COR Biosciences). Relative band signal intensity (BSI) was quantified on Odyssey Image Studio Version 2.0.

*Matrix Metalloproteinase (MMP) Activity*—MMP-2 and MMP-9 activity was assessed by gel zymography as previously described (22). Relative MMP activity was assessed by measuring gelatin lysis area in pixels using Adobe Photoshop CS3 and normalized to the amount of MMP protein detected by immunoblotting.

*Milk Secretion and Milk Composition Analysis*—Milk secretion was carefully assessed by weigh-suckle-weigh as previously described (5) and was calculated as the difference between the final and initial litter weights. Collected milk samples ($n = 5$ dams/genotype) were immediately used to measure the percentage of milk fat by creamatocrit as previously described (5). Frozen milk samples were thawed on ice and centrifuged at 2000 × *g* for 15 min 4 °C to skim. Milk lactose was measured in skimmed milk samples using a lactose assay kit according to manufacturer's instructions (Abcam). Milk β-casein was measured in skimmed milk by immunoblotting as described above and normalized to total milk protein concentration measured by a modified Bradford assay (5).

*Zinc Analysis*—Plasma, tissue, and milk were digested in nitric acid, and zinc concentrations were determined by atomic absorption spectrometry as previously described (23).

*siRNA Transfection of Mammary Epithelial Cells and Secretion Assay*—Mouse MECs (HC11) were a gift from Dr. Jeffery Rosen (Baylor College of Medicine, Houston, TX) and used with the permission of Dr. Bernd Groner (Institute for Biomedical Research, Frankford, Germany). Cells were maintained in growth medium (RPMI 1640 supplemented with 10% fetal bovine serum, 5 μg/ml insulin, 10 ng/ml epidermal growth factor, and gentamycin). Cells were transfected with ZnT2 siRNA (5′-CCAUCUGCCUGGUGU UCAU-3; Sigma) using Lipofectamine 2000 (Life Technologies) as previously described (14) to attenuate ZnT2 (ZnT2KD). Transfected cells were stimulated into a secreting cell with prolactin (1 μg/ml) and cortisol (2 μM) for 24 h. Cell lysates and conditioned medium (CM) were collected and immunoblotted for p-Stat5 or β-casein as described above. The percentage of β-casein secreted was calculated using the following formula: % secreted = (BSI of β-casein in CM)/(BSI of β-casein in CM+BSI of β-casein in lysate) × 100.

*FluoZin-3 Assay*—Transfected HC11 MECs were loaded with FluoZin-3 (Toronto Research Chemicals Inc., Ontario, Canada) as previously described (24) and were viewed by live-cell imaging on the Leica Inverted Confocal Microscope SP8 (Leica Microsystems).

*Statistical Analysis*—Results are presented as the mean ±S.D. Statistical comparisons were performed using Student's *t* test or two-way analysis of variance where appropriate (Prism GraphPad, Berkeley, CA), and a significant difference was demonstrated at $p < 0.05$.

## Results

To understand the role of ZnT2 in mammary gland biology, we used nulliparous adult (10–13 weeks of age) and lactating (LD 10) ZnT2-null (*ZnT2ko*) mice and their wild-type (*wt*) littermates. Briefly, *ZnT2ko* mice were generated by insertion of a neomycin cassette into exon 5 and exon 6 in the *SLC30A2* gene (Fig. 1*A*). The colony was maintained through $ZnT2^{-/+}$ breeding, and progeny were genotyped by PCR followed by DNA agarose gel electrophoresis (Fig. 1*B*). We confirmed successful deletion of ZnT2 in the mammary gland by the absence of ZnT2 protein expression using immunoblotting (Fig. 1*C*) and the absence of ZnT2 staining using immunofluorescence (Fig. 1*D*).

*Nulliparous ZnT2-null Mice Have Reduced Mammary Ductal Invasion and Expansion into the Fat Pad, Impairing Mammary Growth and Development*—To first determine where ZnT2 was expressed in the nulliparous mammary gland, we used immunofluorescence and stained for ZnT2 (Fig. 1*D*). In addition to expression in non-secreting MECs as we have previously shown (13), here we report for the first time that ZnT2 is expressed in macrophages and to a much lesser extent in adipocytes of the stroma in the nulliparous mammary gland. To confirm that ZnT2 was expressed in macrophages, we used immunofluorescence to detect the macrophage marker F4/80 and observed distinct co-localization between ZnT2 and F4/80 (Fig. 1*E*). Interestingly, these macrophages were abnormally activated in *ZnT2ko* mice as indicated by the significant

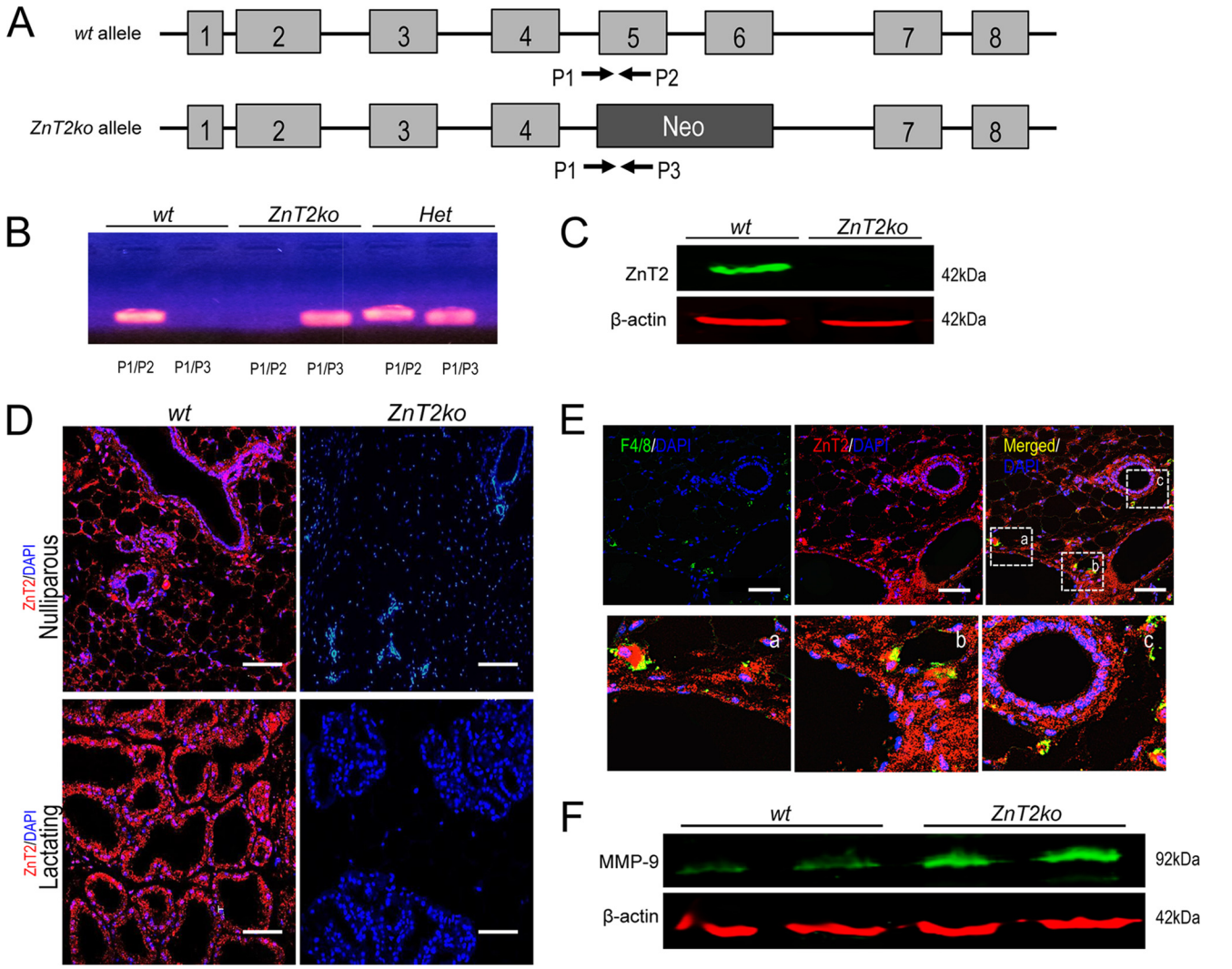


FIGURE 1. **Verification of ZnT2-null genotype and localization of ZnT2 in the mammary gland.** *A*, targeting strategy used to generate the ZnT2-null mice. A neomycin cassette (Neo) was inserted into the *SLC30A2* (ZnT2) gene to eliminate exons 5 and 6; insertion resulted in an Exon5/6 knock-out genotype (*ZnT2ko*). *B*, agarose gel of ZnT2 DNA isolated from ear snips for verification of mouse genotype: *wt* was identified by a product resulting from P1/P2, *ZnT2ko* was identified by a product resulting from P1/P3, and heterozygotes (*Het*) were identified by products resulting from both P1/P2 and P1/P3. *P1*, primer 1; *P2*, primer 2; P3, primer 3. *C*, representative immunoblot of ZnT2 expression (*green*) in total membrane fractions of mammary glands prepared from *ZnT2ko* mice and their wild-type (*wt*) littermates. β-Actin (*red*) served as a loading control. Note the complete absence of ZnT2 in *ZnT2ko* mice. *D*, representative images of ZnT2 (*red*) in the nulliparous (*top*) and lactating (*bottom*) mammary glands of wild type (*wt*) and ZnT2-null (*ZnT2ko*) mice. Nuclei were counterstained with DAPI (*blue*). Note the complete absence of ZnT2 detected in mammary glands from nulliparous and lactating *ZnT2ko* mice. Note the presence of ZnT2 in the MEC of the ducts and alveoli buds and also in the stromal cells in the nulliparous mammary glands. Images of lactating mammary glands, which are naturally depleted of adipocytes, illustrate the substantial amount of ZnT2 expressed in MECs. Magnification, 40×. *Scale bar*, 100 μm. *E*, representative images of ZnT2 (*red*) and F4/80 (*green*, macrophage marker) in mammary glands of wild-type (*wt*) mice. *Boxed areas* in the merged image are enlarged in *a*, *b*, and *c*. Note co-localization (*yellow*) of ZnT2 and F4/80 around epithelial cells of ducts and alveoli buds. *F*, representative immunoblot of MMP-9 expression (*green*) in mammary glands from *wt* and *ZnT2ko* mice. β-Actin (*red*) served as a loading control.

increase in MMP-9 expression in the mammary gland (Fig. 1*F*; Ref. 25). Importantly, there was no significant effect on plasma (*wt*, 12.13 μmol/liter ± 1.4; *ZnT2ko*, 11.14 μmol/liter ± 1.9), liver (*wt*, 29.33 μg Zn/g of tissue ± 3.2; *ZnT2ko*, 28.07 μg Zn/g of tissue ± 3.1) or mammary gland (*wt*, 11.44 μg Zn/g of tissue ± 1.3; *ZnT2ko*, 11.15 μg Zn/g of tissue ± 1.8) zinc concentrations.

To assess the effects of a ZnT2-null phenotype on the nulliparous mammary gland, we examined the morphology of the mammary glands taken from nulliparous mice by whole-mount analysis and histology. Mammary glands from nulliparous *ZnT2ko* mice showed no gross defects in alveolar bud formation; however, both primary and secondary ducts had reduced invasion and expansion into the surrounding mammary fat pad, indicated by the reduction in ductal length and lateral branching, respectively (Fig. 2, *A*–*C*). As a result, the relative ratio of glandular tissue to stromal area was significantly lower in the mammary glands of *ZnT2ko* mice (0.67 ± 0.03) compared with *wt* littermates (0.80 ± 0.07; $p < 0.05$). Consistent with a lower glandular/stromal area, images of H&E-stained mammary gland sections (Fig. 2*D*) documented significantly fewer ducts in *ZnT2ko* mice (10 ducts/field of view ± 2) compared with *wt* littermates (22 ducts/field of view ± 1; $p < 0.005$), and these ducts were generally collapsed. Also noted in the H&E images was the expansion of adipocyte size in *ZnT2ko* mice (discussed below). To determine if these effects were associated with

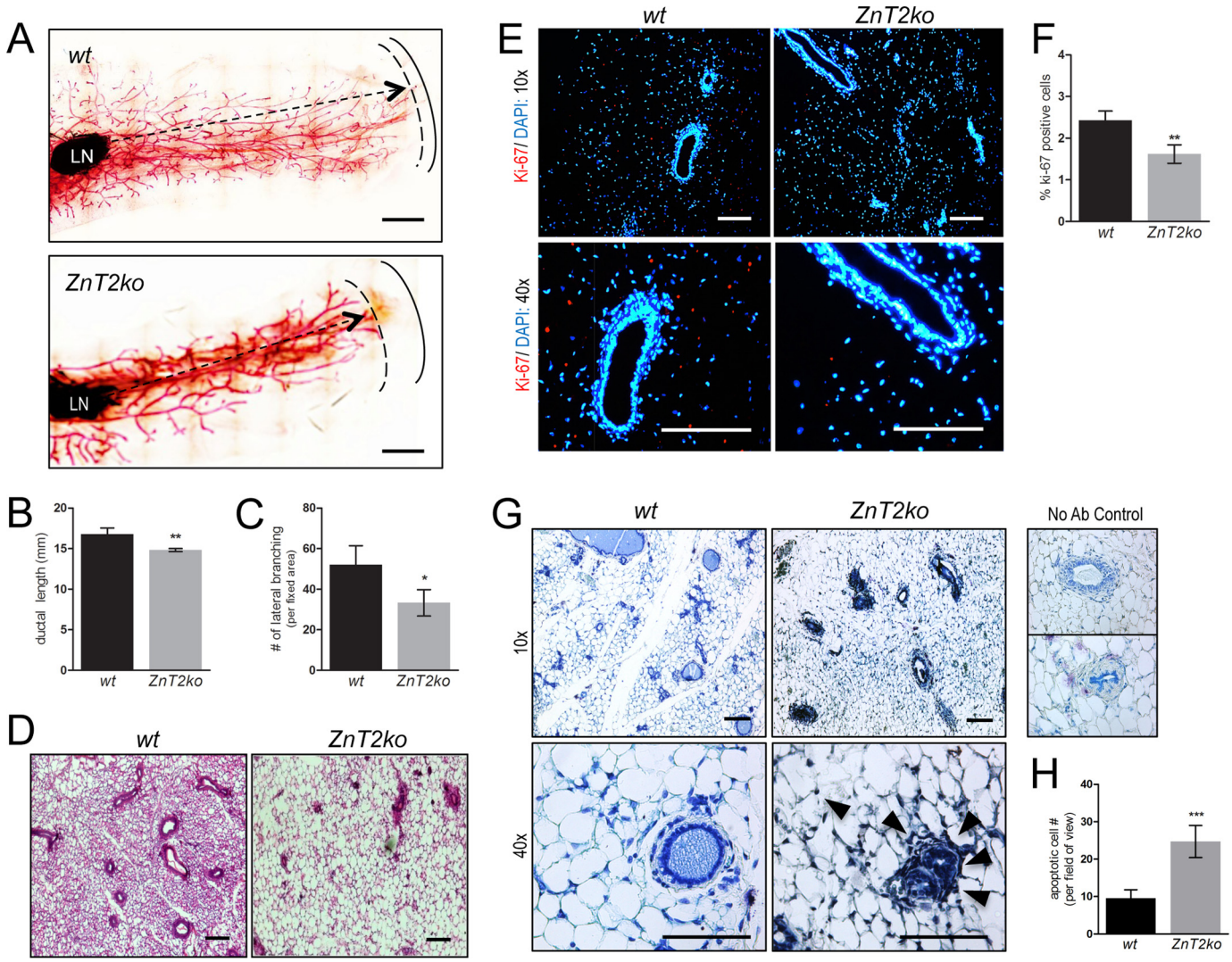


FIGURE 2. **Mammary gland invasion and expansion is impaired in ZnT2-null mice during development.** *A*, representative images of whole mount analysis of mammary glands from nulliparous wild-type (*wt*) and ZnT2-null (*ZnT2ko*) mice. *Arrows* illustrate the ductal length from the lymph node (*LN*). *Solid* and *dotted lines* outline the fat pad and end of the ducts, respectively. Magnification, 4x (stitched images). *Scale bar*, 2 mm. *B*, quantification of ductal length in mammary glands from nulliparous *wt* and *ZnT2ko* mice. Data represent the mean ± S.D., $n = 3$ mice/genotype; **, $p < 0.01$. *C*, number of lateral branches in a fixed area of whole mount images. Data represent the mean ± S.D., $n = 3$ mice/genotype; *, $p < 0.05$. *D*, representative image of H&E-stained mammary gland sections from nulliparous *wt* and *ZnT2ko* mice. Note the lack of ducts, the collapsed ducts, and the larger adipocyte size in *ZnT2ko* compared with *wt* mice. Magnification, 10×. *Scale bar*, 200 μm. *E*, representative images of Ki-67 positive nuclei (*red*) in mammary gland sections from nulliparous *wt* and *ZnT2ko mice.* Nuclei were counterstained with DAPI (*blue*). Magnification, 10× (*top*), 40× (*bottom*). *Scale bar*, 100 μm. *F*, data represent the mean number of Ki-67$^+$ cells ±S.D. in one 10× field; $n = 3$ mice/genotype; **, $p < 0.01$. *G*, representative images of TUNEL staining in mammary gland sections from nulliparous *wt* and *ZnT2ko* mice, counterstained with toluene blue. Note the presence of TUNEL-positive cells (*arrowheads*) in *ZnT2ko* compared with *wt*. No antibody (*Ab*) controls were not incubated with the TUNEL reaction mixture. Magnification, 10× (*top*), 40× (*bottom*). *Scale bar*, 100 μm. *H*, data represent the mean number of apoptotic cells ±S.D. in five 40× fields of view per section; $n = 3$ mice/genotype; ***, $p < 0.001$.

reduced cell proliferation, we counted the number of nuclei that were stained positive for Ki-67 and found that the number of Ki-67-positive cells in the stroma of *ZnT2ko* mice was significantly lower compared with *wt* mice (Fig. 2, *E* and *F*). Moreover, apoptotic cells were identified using the TUNEL assay and were frequently detected around the ductal cells in the mammary glands of *ZnT2ko* mice (Fig. 2, *G* and *H*). Collectively, this indicates that loss of ZnT2 function resulted in a hypoplastic mammary gland phenotype in nulliparous adult mice.

To explore mechanisms through which the loss of ZnT2 impaired ductal expansion, we first measured the activity and expression MMP-2, a zinc-dependent enzyme that is activated in vesicles (26, 27) and is known to be critical for ductal cell proliferation and the process of ductal elongation (22, 28). Consistent with defects in ductal elongation, the mammary glands of ZnT2-null mice had reduced MMP-2 activity without changes in MMP-2 protein abundance (Fig. 3, *A* and *B*; Ref. 22), suggesting that the loss of ZnT2 reduced zinc availability for MMP-2 activation. Reduced MMP-2 activity was consistent with the substantial increase in collagen deposition around collapsed ducts in the mammary glands of *ZnT2ko* mice (Fig. 3*C*; Ref. 29). Alternatively, alterations in the stromal environment can affect ductal expansion (30). Consistent with a potential effect of the stromal environment, an interesting finding we noted was that the adipocytes in the mammary glands of *ZnT2ko* mice were ~4× larger (7070 $\mu m^2$ ±4624) compared with the adipocytes in *wt* littermates (1770 $\mu m^2$ ± 33; $p < 0.05$) with no effect on the overall size of the mammary gland (data

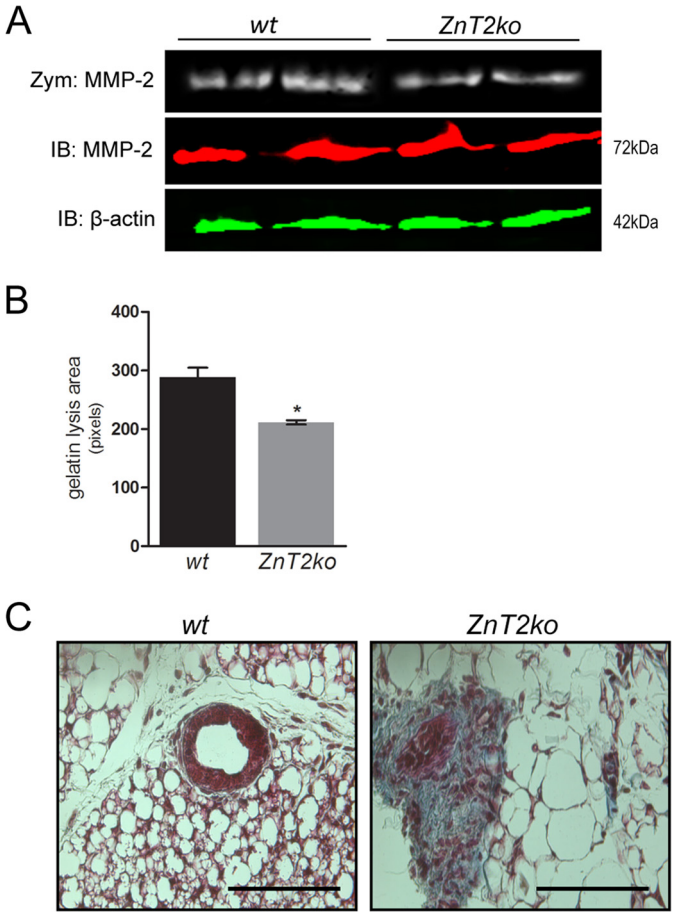


FIGURE 3. **ZnT2 loss reduces MMP-2 activity and increases collagen deposition.** *A*, evaluation of MMP-2 activity by gelatin zymography (*Zym*; *cleared bands*) and MMP-2 expression (*red*) by immunoblotting (*IB*) in mammary glands from wild-type (*wt*) and ZnT2-null (*ZnT2ko*) mice. β-Actin (*green*) served as a loading control. *B*, data represent mean gelatin lysis area ±S.D.; $n = 4$ mice/genotype; *. $p < 0.05$. The experiment was repeated twice. *C*, representative image of trichrome staining of mammary gland sections from nulliparous *wt* and *ZnT2ko* mice. Note the increase in collagen deposition (*blue*) around the collapsed ducts in *ZnT2ko* mice that was not present in *wt* mice. Magnification, 40×. *Scale bar*, 100 μm.

not shown). Collectively, these data indicate that the loss of ZnT2 impaired ductal invasion and expansion into the mammary fat pad.

*Lactating ZnT2-null Mice Accumulate Zinc and Have Profound Defects in Morphology and Impaired MEC Differentiation*—Consistent with results in nulliparous *ZnT2ko* mice and previous reports in breastfeeding women with heterozygous mutations in ZnT2 (11, 17), overall zinc status as measured by plasma (*wt*, 13.08 μmol/liter ± 1.4; *ZnT2ko*, 13.95 μmol/liter ± 1.3) and liver (*wt*, 32.38 μg Zn/g of tissue ± 2.6; *ZnT2ko*, 31.78 μg Zn/g of tissue ± 4.5) zinc concentration was not altered in the lactating *ZnT2ko* mice. Additionally, similar to previous reports in rats and mice (31, 32), ZnT2 was localized intracellularly and associated with the apical membrane of MECs in the mammary gland during lactation (Fig. 1*D*). As observed previously (32, 33), the zinc concentration in the mammary gland was higher during lactation compared with the non-lactating state, and this relationship was not affected by loss of ZnT2 (Fig. 4*A*). However, we noted that during lactation, *ZnT2ko* mice accumulated ~30% more zinc in the mammary gland compared with *wt* littermates. Because zinc accumulation is cytotoxic and is buffered by either increasing expression of ZnT2 for sequestration into vesicles or increasing expression of metallothionein (MT) for sequestration in the cytoplasm (9, 34), we measured expression of MT as a proxy for cytoplasmic zinc accumulation. We found that without the ability to sequester zinc via ZnT2 in *ZnT2ko* mice, there was a ~7-fold increase in MT expression in the mammary gland (Fig. 4*B*), suggesting that loss of ZnT2 results in zinc accumulation in the cytoplasm. To verify this, we performed a histological zinc stain using Zinpyr-1 (*ZP-1*), which is a cell-permeable fluorescent probe selective for labile zinc, and confirmed that the loss of ZnT2 impairs zinc vesicularization and accumulates zinc in the cytoplasm of the mammary epithelium (Fig. 4*C*). To determine if the increase in zinc accumulation in the mammary glands of ZnT2-null mice was specific to loss of ZnT2 in MECs, we transfected HC11 cells with ZnT2 siRNA (ZnT2KD) and loaded with FluoZin-3, a zinc-specific fluorophore that fluoresces upon zinc binding. Again, the loss of ZnT2 in MECs impaired zinc vesicularization and increased cytoplasmic zinc (Fig. 4*D*).

We next examined the mammary glands of lactating ZnT2-null mice using whole-mount analysis. Images of the mammary gland from lactating *wt* mice illustrated a fully differentiated mammary gland with the expected depletion of adipocytes and development of mature alveoli (Fig. 5*A*). In contrast, the mammary glands of lactating *ZnT2ko* mice had markedly less lobuloalveolar expansion (Fig. 5*B*). Consistent with these defects, H&E-stained sections revealed a profound reduction in alveoli with abnormal preservation of adipose in the stroma of *ZnT2ko* mice, which was absent in the mammary glands of *wt* mice (Fig. 5, *C* and *D*). Under higher magnification, defects in the alveoli of *ZnT2ko* mice were more clearly observed. w*t* mice had well expanded alveoli surrounded by flat MECs and lumens filled with lipid droplets, hallmarks of a well differentiated and actively secreting mammary gland (Fig. 5*E*; Refs. 35 and 36). In contrast, *ZnT2ko* mice had constricted alveoli, and the MECs lining the alveoli were swollen with an accumulation of lipid-laden and proteinaceous material and an absence of active lipid droplet fusion at the apical membrane as seen in the *wt* mice (Fig. 5*F*). The irregular shape and narrow distention of the alveolar lumen, determined by the significant reduction of alveolar circularity in lactating *ZnT2ko* mice (Fig. 5, *G* and *H*), suggested impaired alveologenesis (37).

To determine if mammary gland defects during lactation were associated with enhanced cell turnover, we analyzed apoptosis and cell proliferation by TUNEL and Ki-67 staining, respectively. Apoptotic cells were profoundly evident in the mammary epithelium and alveolar lumen of mammary glands from *ZnT2ko* mice (Fig. 6, *A* and *B*), which were not present in the mammary glands from *wt* littermates. Interestingly, mammary glands from lactating *ZnT2ko* mice also had a significantly greater number of proliferating MECs compared with *wt* mice (Fig. 6, *C* and *D*), consistent with an increase in cell turnover. Because the mammary gland undergoes profound cell turnover at the time of weaning or involution (38, 39), we next determined if increased cell turnover in response to the loss of ZnT2 function was a consequence of premature involution by measuring the abundance of phosphorylated Stat3 (p-Stat3) (40).

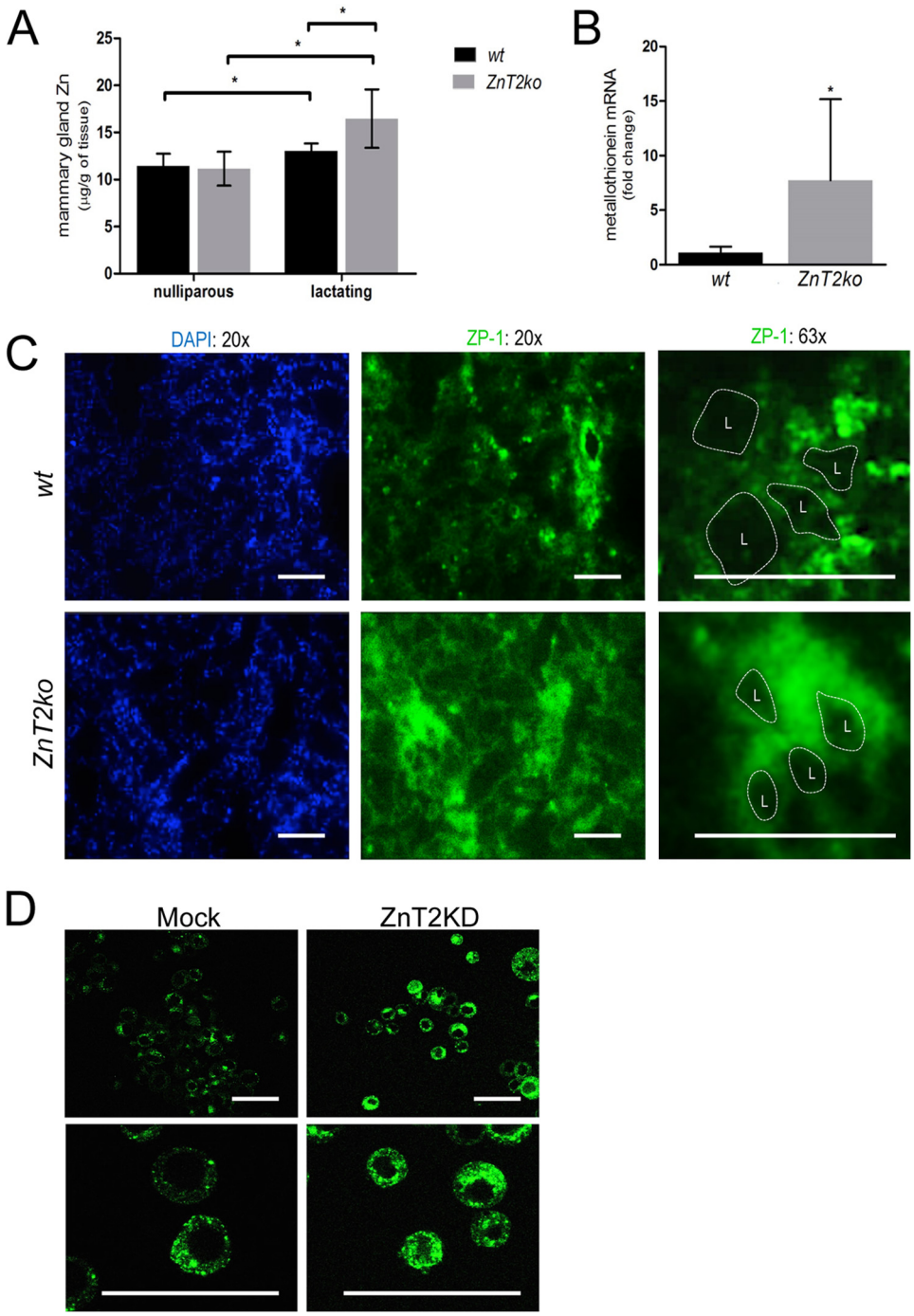


FIGURE 4. **Loss of ZnT2 inhibits $Zn^{2+}$ vesicularization and increases cytoplasmic $Zn^{2+}$ in the mammary epithelium during lactation.** *A*, zinc concentration was measured in mammary gland by atomic absorption spectroscopy in wild-type (*wt*) and ZnT2-null (*ZnT2ko*) mice. Data represent the mean mammary gland ($\mu$g of Zn/g of tissue) $\pm$S.D. (*wt* $n = 6$ and *ZnT2ko* $n = 4$) $Zn^{2+}$ concentration in nulliparous and lactating mammary glands; *, $p < 0.05$. *B*, expression of MT in the mammary gland of lactating *wt* and *ZnT2ko* mice. Data represent mean -fold change in MT expression of *ZnT2ko* mice relative to *wt* $\pm$S.D.; *wt* $n = 7$ and *ZnT2ko* $n = 5$; *, $p < 0.05$. *C*, representative images of Zinpyr-1 (*ZP-1*) fluorescence (*green*) in frozen mammary gland sections from lactating *wt* and *ZnT2ko* mice. Nuclei were counterstained with DAPI (*blue*). Note the lack of punctate zinc fluorescence and the accumulation of zinc fluorescence in the mammary epithelium of *ZnT2ko* mice. *Dotted lines* outline the alveolar lumen (*L*). Magnification, 20$\times$ (*left*), 63$\times$ (*right*). *Scale bar*, 200 $\mu$m. *D*, representative images of Fluozin-3 fluorescence staining in mock-transfected (*Mock*) and ZnT2-attenuated (*ZnT2KD*) MECs. Note punctate vesicular zinc staining in mock and hazy cytoplasmic zinc staining in ZnT2KD. *Scale bar*, 50 $\mu$m.

We found no expression of p-Stat3 in the lactating mammary glands of either *ZnT2ko* or *wt* mice (Fig. 6*E*), excluding the possibility that loss of ZnT2 function spontaneously activates premature involution.

Next, we measured the abundance of phosphorylated Stat5 (p-Stat5) to determine if the loss of ZnT2 impaired mammary gland differentiation (41). Strikingly, we found a significant loss of p-Stat5 expression with no change in total Stat5 expression in the mammary glands of lactating *ZnT2ko* mice (Fig. 6*F*), suggesting that loss of ZnT2 reduced Stat5 activation (Fig. 6*G*) and mammary gland differentiation (42). To determine if the loss of differentiation observed in the mammary glands of lactating

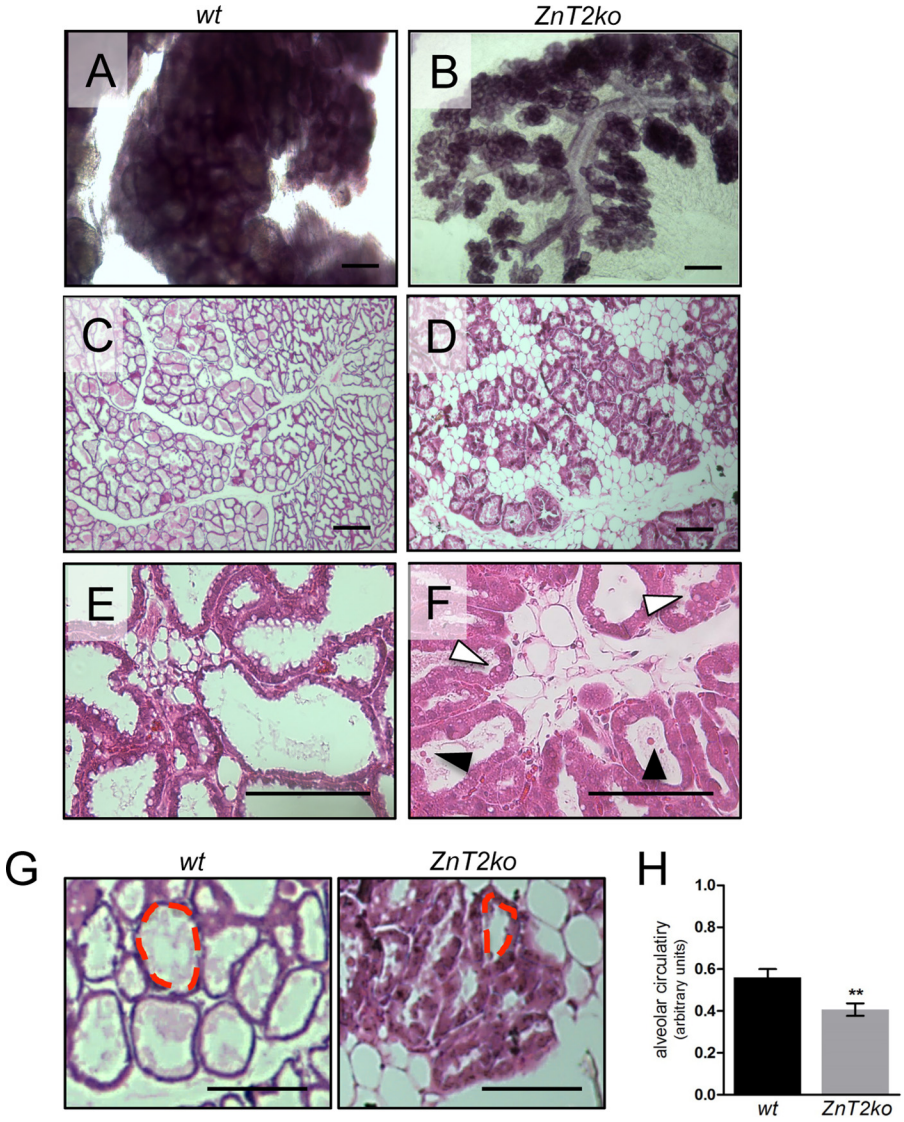


FIGURE 5. **Lactating ZnT2-null mice have morphological defects in the mammary gland.** Whole mount analysis of mammary glands from lactating wild-type (*wt*; A) and ZnT2-null (*ZnT2ko*;B) mice is shown. Note the sparse alveolar structures in *ZnT2ko* compared with *wt* mice. Magnification, 4×. *Scale bar*, 200 μm. H&E-stained sections of mammary gland from lactating *wt* (*C* and *E*) and *ZnT2ko* (*D* and *F*) mice. Note the lack of alveoli and disorganization of alveolar structures, preserved adipocytes, and swollen MECs of *ZnT2ko* mice (*D*). Note the distended MECs lining the alveoli and lipid droplet accumulation in MEC (*white arrowheads*) and apoptotic cells (*black arrowheads*) in the alveolar lumen of *ZnT2ko* mice (*F*). Magnification, 10×. *Scale bar*, 100 μm (*C* and *D*); magnification, 40×. *Scale bar*, 100 μm (*E* and *F*). *G*, analysis of structural irregularity of alveoli in mammary glands from lactating *wt* and *ZnT2ko* mice, as measured by the alveolar circularity (0–1 arbitrary units). A representative image of H&E-stained mammary gland sections from lactating *wt* and *ZnT2ko* mice is shown. The *dotted line* illustrates alveolar circularity. Magnification, 40×. *Scale bar*, 200 μm. *H*, data represent mean alveolar circularity ±S.D., taken from 40 alveoli/mouse from $n = 3$ mice/genotype; **, $p < 0.01$.

ZnT2-null mice was specific to loss of ZnT2 in MECs, we transfected HC11 cells with ZnT2 siRNA (ZnT2KD) and differentiated them with PRL to activate p-Stat5 signaling (43). These data showed that differentiation was impaired in ZnT2KD MECs as both p-Stat5 (Fig. 7*A*) and β-casein expression and secretion (Fig. 7, *B–D*) were significantly reduced in ZnT2-attenuated MECs. Thus, consistent with our observations in lactating mice, the loss of ZnT2 in MECs impaired differentiation and secretion, implicating ZnT2 as a critical regulator of mammary gland function during lactation.

*ZnT2-null Mice Have Defects in Subcellular Organization*—In light of the observation that loss of ZnT2 function compromised differentiation, we next visualized the lactating mammary glands using transmission electron microscopy to further characterize the consequence of a ZnT2-null phenotype at the subcellular level. Transmission electron microscope images revealed that in lactating *wt* mice, the alveoli were lined with polarized MECs that had a defined basal membrane (Fig. 8*A*) and an apical membrane with extended microvilli and tight junctions connecting the cells (Fig. 8*C*). These MECs were normally filled with endoplasmic reticulum and contained well organized Golgi apparatus and mitochondria that were oriented around a spherical nucleus (Fig. 8, *A*, *D*, and *E*; Ref. 44), which together regulate the secretion of milk constituents across the apical membrane. Moreover, secretory vesicles containing casein micelles and fused lipid droplets were directed toward the apical membrane, indicating active milk secretion (Fig. 8, *F* and *G*). In stark contrast, the MECS of ZnT2-null mice

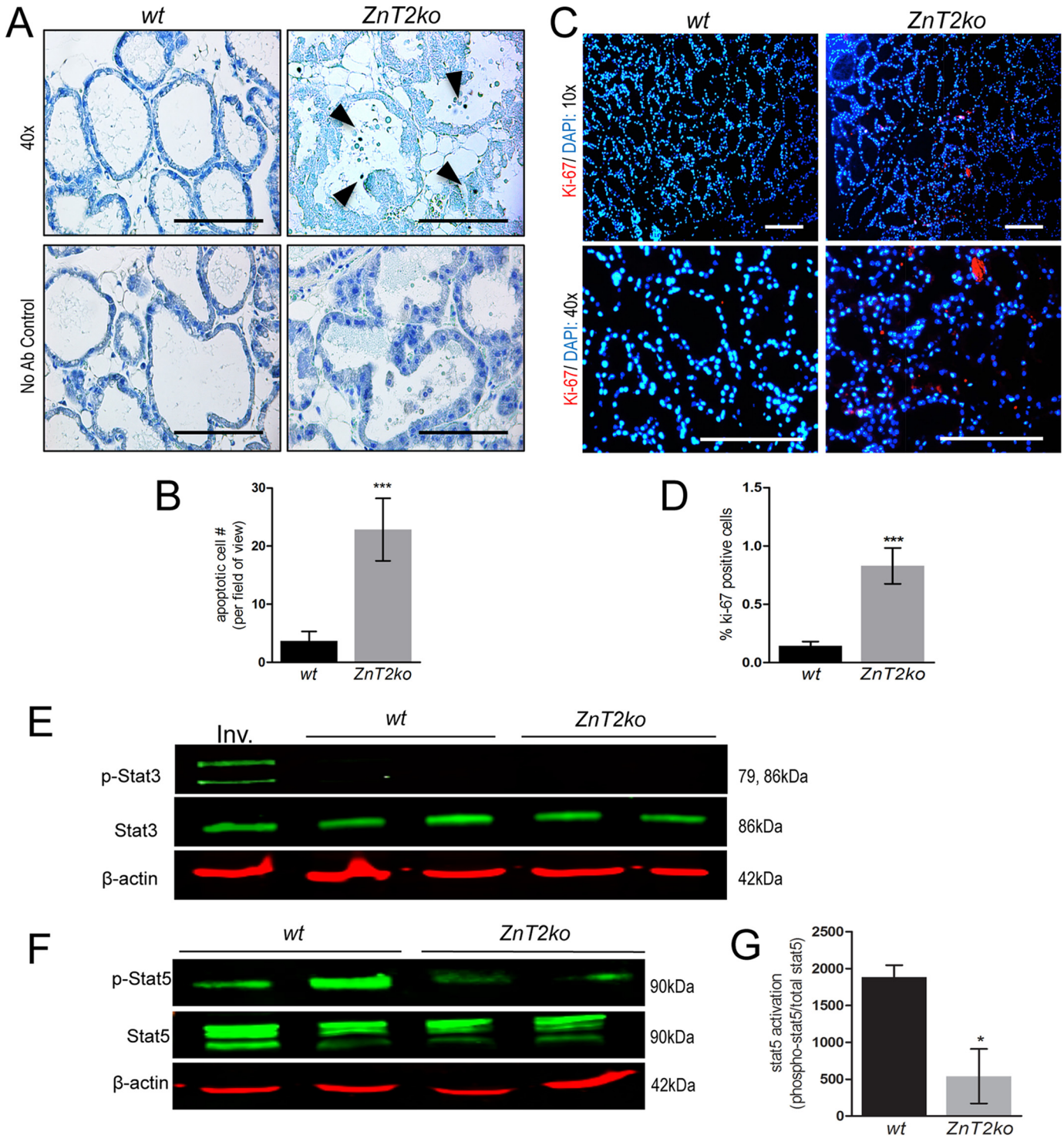


FIGURE 6. **Lactating ZnT2-null mice have increased cell turnover due to impaired lactational differentiation.** *A*, representative images of TUNEL in sections of mammary gland from lactating wild-type (*wt*) and ZnT2-null (*ZnT2ko*) mice, counterstained with toluene blue. No antibody (*Ab*) controls were not incubated with TUNEL reaction mixture. Note the presence of TUNEL-positive cells and the extrusion of TUNEL-positive cells into the alveolar lumen (*arrowhead*) in *ZnT2ko* mice. Magnification, 40×. *Scale bar*, 100 μm. *B*, data represent the mean number of apoptotic cells ±S.D. in five 40× fields of view per section; $n = 3$ mice/genotype; ***, $p < 0.001$ *C*, representative images of Ki-67 positive nuclei (*red*) in mammary gland sections from lactating *wt* and *ZnT2ko* mice. Nuclei were counterstained with DAPI (*blue*). Magnification, 10× (*top*), 40× (*bottom*). *Scale bar*, 100 μm. *D*, data represent the mean number of Ki-67$^+$ cells ±S.D. in one 10× field; $n = 3$ mice/genotype; ***, $p < 0.001$. *E*, representative immunoblot of p-Stat3 (*green*), a marker of involution, and total Stat3 (*green*) expression in cell lysates of mammary glands from lactating wild-type (*wt*) and ZnT2-null (*ZnT2ko*) mice. Involuting mammary gland (*Inv.*) served as a positive control. Stat3 (*green*) and β-actin (*red*) served as a loading control. Note the absence of p-Stat3 expression in both the lactating *wt* and *ZnT2ko* mice. *F*, representative immunoblot of p-Stat5 (*green*) in cell lysates from mammary glands from lactating *wt* and *ZnT2ko* mice. Total Stat5 (*green*) and β-actin (*red*) served as loading controls. *G*, quantification of Stat5 activation. Data represent the mean p-Stat5/total Stat5 ratio ±S.D., $n = 4$ mice/genotype; *, $p < 0.05$. The experiment was repeated twice.

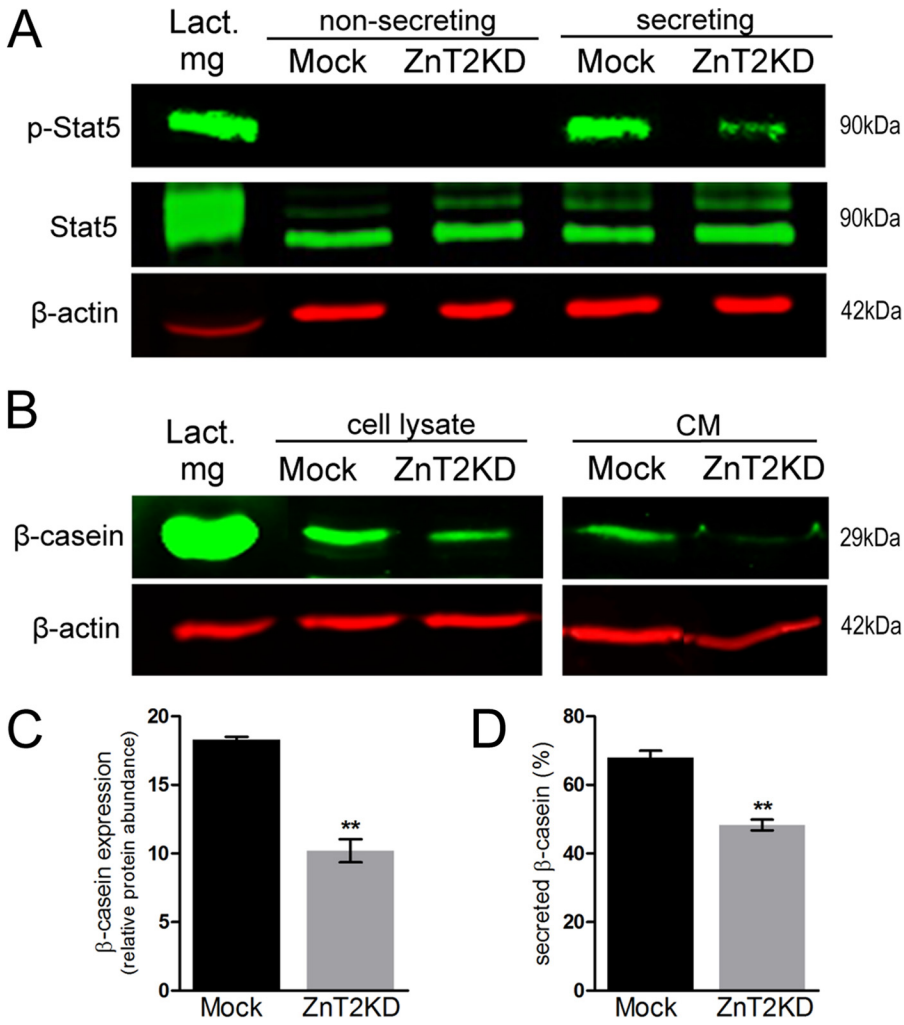


FIGURE 7. **ZnT2 attenuation impairs differentiation, milk production, and secretion in MECs *in vitro*.** *A*, representative immunoblot of p-Stat5 (*green*) in cell lysates of non-secreting and secreting mock-transfected (*Mock*) and ZnT2-attenuated (*ZnT2KD*) MECs. Lactating mammary glands (*Lact. mg*) served as a positive control. Total Stat5 (*green*) and β-actin (*red*) served as loading controls. *B*, representative immunoblot of β-casein (*green*) in cell lysates and CM of Mock and ZnT2KD MECs. Lactating mammary glands (*Lact. mg*) served as a positive control, and β-actin (*red*) served as a loading control. *C*, quantification of β-casein expression in cell lysates of mock and ZnT2KD MECs. Data represent mean protein abundance normalized to total protein (band intensity/μg of protein) ±S.D., $n = 3$ samples/group; **, $p < 0.01$. *D*, percentage of β-casein that was secreted and calculated using the following formula: % secreted = (BSI of β-casein in CM)/(BSI of β-casein in CM+BSI of β-casein in lysate). Data represent the mean secreted β-casein (%) ±S.D., $n = 3$ samples/group; **, $p < 0.01$.

were severely disorganized, lacking a distinct cell-cell junctions and presented with numerous pseudolumina (Fig. 8*B*), similar to the morphology seen in Stat5-null mice with impaired MEC differentiation (45). Most notable were the disturbed apical membrane (Fig. 8*H*), swollen mitochondria (Fig. 8*I*) and fragmented endoplasmic reticulum (Fig. 8*J*) that were scattered throughout the cell. Frequently, we detected secretory vesicles that did not properly package casein micelles, which were dispersed throughout the cytosol (Fig. 8*K*). Moreover, lipid droplets failed to fuse for secretion into the lumen as milk fat globules and instead accumulated inside the cell (Fig. 8*L*). Collectively, these observations confirm impaired MEC differentiation in the *ZnT2ko* mice and provide evidence that the loss of ZnT2 function in MECs disrupts secretory activation and cellular secretion processes during lactation.

*Milk Secretion Is Impaired in ZnT2-null Dams, Altering Milk Composition and Affecting Pup Survival*—Consistent with reduced milk zinc secretion in women who have mutations in ZnT2 (11, 16–18), ZnT2-null mice had an ~30% reduction in milk zinc concentration (Fig. 9*A*). Because women with mutations in ZnT2 have a much greater (50–90%) reduction in milk zinc concentration (10, 11, 13, 16, 17), we expected to see a greater loss of zinc transfer into milk in *ZnT2ko* mice. Given this unexpected finding, we tested the hypothesis that ZnT4 expression was augmented to compensate for the lack of ZnT2, as we and others (24, 46) have shown that ZnT4 is important for zinc secretion into milk. However, we found that ZnT4 abundance was actually lower in the mammary glands from *ZnT2ko* mice (data not shown), eliminating a compensatory response as an alternative explanation. Intriguingly, we found that alterations in milk composition extended well beyond reduced zinc concentration in *ZnT2ko* mice. We found that the concentrations of major milk components, β-casein, fat, and lactose, were also significantly reduced by ~30–40% in the milk collected from ZnT2-null dams (Fig. 9, *B–D*). Moreover, milk secretion was severely impaired in lactating ZnT2-null dams during both early (~25% less) and peak (~30% less) lactation periods (Fig. 9*E*). As a result, ~50% of ZnT2-null dams failed to maintain

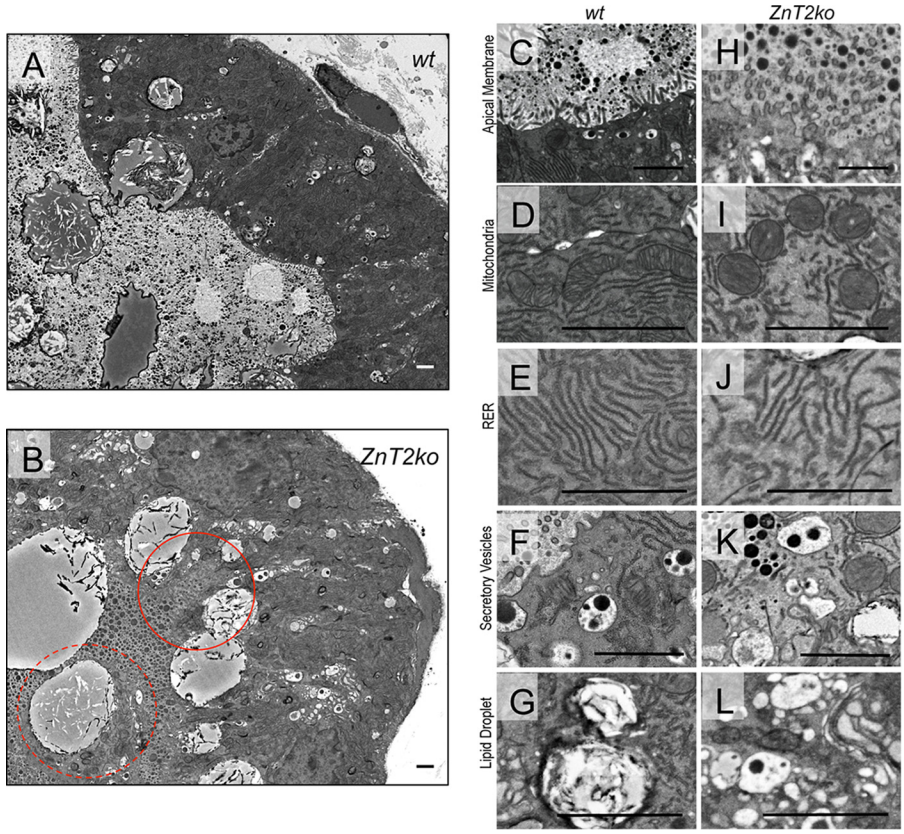


FIGURE 8. **Lactating ZnT2-null mice have defects in MEC substructure.** Transmission electron micrographs of mammary glands from lactating wild-type (*wt*) (*A*) and ZnT2-null (*ZnT2ko*) (*B*) mice. Magnification, 500×; *scale bar* = 2 μm. Note the formation of pseudolumina on the apical membrane (*circle*) and the presence of apoptotic cells in the alveolar lumen (*dotted circle*) in sections from *ZnT2ko* mice. Enlarged images of subcellular structures: apical membrane (*C* and *H*), mitochondria (*D* and *I*), rough endoplasmic reticulum (*RER*; *E* and *J*), secretory vesicles (*F* and *K*) and lipid droplets (*G* and *L*) in *wt* (*C–G*) and *ZnT2ko* (*H–L*) mice. *Scale bar*, 2 μm.

their litters up to LD10 (Fig. 9*F*) and had a significantly lower litter survival rate (*ZnT2ko*, 53.9% ± 45.7 *versus wt*, 92.9% ±14.1; $p < 0.05$). These data demonstrate that the ZnT2 is a critical regulator of mammary gland differentiation and milk secretion during lactation, which is crucial for sustaining infant health.

## Discussion

ZnT2 is expressed in the mammary gland (47), and previous studies have focused on its role in importing zinc into vesicles (10, 13) for secretion into milk during lactation (11, 16, 17). ZnT2 is also found in mitochondria and vesicles in non-lactating mammary glands; however, the physiological role of ZnT2-mediated zinc transport beyond that of zinc secretion into milk is almost entirely unknown. Here, we found that ZnT2 is critical for normal mammary gland development and function during lactation. Using nulliparous and lactating ZnT2-null mice, we demonstrate that the loss of ZnT2 1) impaired mammary expansion during development, 2) reduced mammary gland differentiation and impaired secretion during lactation, and 3) compromised milk composition and offspring survival.

*The Role of ZnT2-mediated Zinc Transport in Mammary Expansion*—Non-lactating ZnT2-null mice had profound defects in mammary development and ductal expansion. During puberty, the mammary gland undergoes key developmental phases including terminal end bud formation, ductal elongation, and ductal branching that collectively establish a branching network of parenchymal ducts surrounded by a supporting adipose and stroma (48). One explanation for impaired mammary development may be alterations in zinc-dependent functions. A key observation from our study is that MMP-2 activity was decreased, suggesting that the inability to vesicularize zinc resulted in cytoplasmic zinc accumulation and buffering by MT, perhaps withholding zinc from activating MMP-2 within vesicles for ductal invasion into the stromal tissue (49–51). An alternative explanation may reflect mitochondrial dysfunction as ZnT2 transports zinc across the inner mitochondrial membrane and regulates apoptosis (15), a key mechanism critical for ductal expansion in the mammary gland (52). Consistent with this postulate, we noted greater apoptotic activity in MECs and significantly fewer mammary ducts in ZnT2-null mice. This suggests that either mitochondrial zinc depletion or cytoplasmic zinc accumulation may have perturbed closure of the mitochondrial permeability transition pore (53) and, thereby, induced release of apoptotic-inducing factors that disrupt ductal expansion. Further studies on mitochondrial function are required to understand these defects.

In addition to MECs, the stroma, which includes adipocytes and macrophages, is crucial for mammary gland development by facilitating epithelial-mesenchymal interactions for branching morphogenesis and ductal outgrowth (30, 54). An unex-

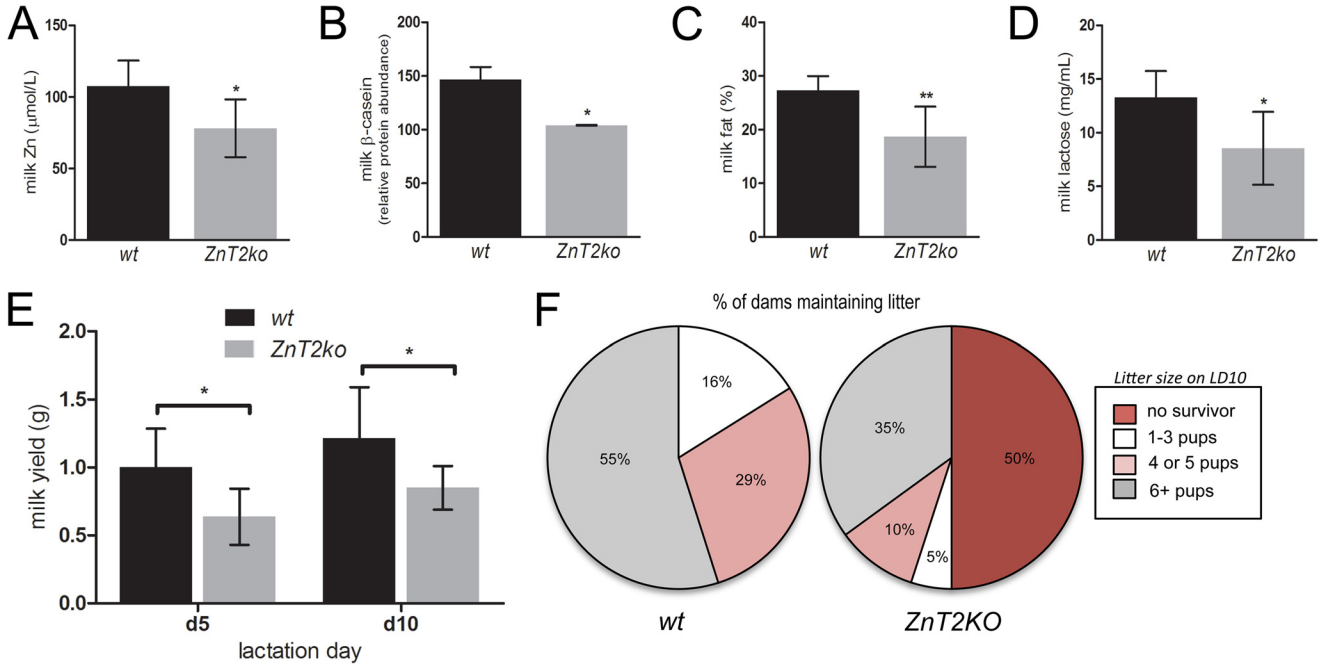


FIGURE 9. **Compromised milk secretion in lactating ZnT2-null dams affect offspring survival.** *A*, quantification of zinc concentration in milk from lactating wild-type (*wt*) and ZnT2-null (*ZnT2ko*) mice. Data represent the mean milk zinc concentration (μmol/liter) ±S.D., $n = 5$ mice/genotype; *, $p < 0.05$. *B*, quantification of β-casein levels in milk from lactating *wt* and *ZnT2ko* mice. Data represent the mean β-casein abundance normalized to total protein level (BSI/μg of protein) ±S.D., $n = 5$ mice/genotype; *, $p < 0.05$. *C*, quantification of fat levels in milk from lactating *wt* and *ZnT2ko* mice. Data represent mean fat (%) ±S.D., $n = 5$/genotype; **, $p < 0.01$. *D*, quantification of lactose concentration in milk from *wt* and *ZnT2ko* mice. Data represent mean milk lactose concentration (mg/ml) ±S.D., *wt* $n = 10$ mice and *ZnT2ko* $n = 5$ mice; *, $p < 0.05$. *E*, milk volume calculated as the difference between litter weight before and after suckling on LD5 and LD10 in wild-type (*wt*) and ZnT2-null (*ZnT2ko*) mice. Data represent mean milk yield (g) ±S.D. *wt* $n = 10$ litters, and *ZnT2ko* $n = 5$ litters); *, $p < 0.05$. *F*, pie graph of the percentage of dams maintaining the indicated litter size at LD10: *no survivor*, 1–3 pups, 4 or 5 pups and 6+ pups. Note the large percentage (~50%) of *ZnT2ko* dams failing to maintain a litter up to LD10.

pected finding from our study was that ZnT2 was expressed in macrophages and adipocytes. Consequently, the loss of ZnT2 in these cells may also affect optimal development of the ductal tree. Adipocytes dictate the extent of which the glandular tissue develops into a functional branching network in the mammary gland (55) by secreting leptin and other endocrine factors that contribute to paracrine interactions with ductal epithelial cells (56); thus, enhanced adipocyte mass may affect these interactions. Moreover, zinc has insulin-like effects in adipocytes, stimulating lipogenesis and increasing fatty acid accumulation (57, 58). Consistent with effects of adipocyte zinc accumulation, we observed adipocyte hypertrophy in ZnT2-null mammary glands, which could indicate increased lipogenesis (59). Therefore, the loss of ZnT2 in adipocytes may mirror insulin-like effects on lipogenesis that stunt ductal growth (60) or may affect the synthesis or release of paracrine factors, such as adiponectin and collagen VI (61) from adipocytes that initiate epithelial/mesenchymal interaction and facilitate ductal expansion (55). Finally, macrophages are also important for mammary gland development, as they are recruited to the epithelial cells to support proliferation for ductal outgrowth (30, 62) by supplying growth factors, cytokines, and chemokines (63) or by engulfing apoptotic cells that interfere with epithelial proliferation (64). The lack of cell proliferation in ZnT2-null mice suggests that loss of ZnT2 in macrophages may not be able to support normal epithelial and fibroblast proliferation. Because MMP-9 expression was greater in ZnT2-null mice, one explanation may be that the loss of ZnT2 hyperactivates macrophages (25), which can stimulate tumor growth factor-β signaling pathway and impair ductal outgrowth (65, 66). Additionally, adipocyte hypertrophy combined with abnormal macrophage activation may be indicative of an inflammatory mammary gland that in turn interrupts optimal mammary development (67, 68). Further studies are required to understand the role of ZnT2-mediated zinc transport in the stromal cells in the mammary gland.

*ZnT2 Is Critical for Mammary Differentiation during Lactation*—It is possible that defects in mammary gland development persist through pregnancy, affecting morphological development and differentiation. However, we chose to focus on the loss of ZnT2 function on the lactating mammary gland as previous studies clearly show that ZnT2 imports zinc into secretory vesicles, thus playing a vital role in zinc secretion into milk during lactation (10, 13, 16, 17). Although milk zinc concentration was significantly reduced in ZnT2-null mice, much more profound was the accumulation of zinc and the morphological defects observed in the lactating mammary glands that indicate impaired mammary differentiation. Mammary gland differentiation, milk production, and active secretory mechanisms during lactation (69) are primarily activated by prolactin-induced Stat5 signaling. Here, we noted that loss of ZnT2 reduced p-Stat5 in the mammary gland and MECs *in vitro*, indicating that differentiation was dramatically impaired (41, 70). The loss of ZnT2-mediated zinc transport into vesicles may activate zinc-dependent dephosphorylation enzymes in the cytoplasm, such as Shp-2 (71), or inhibit prolactin signaling through aberrant stimulation or suppression of factors that regulate Stat5 activity, such as ErbB4, Pak1, caveolin-1, Socs2, Id2,

and Elf5 (70). Notably, functional and morphological defects in ZnT2-null mice were consistent with compromised MEC polarity, tight junction formation, and cellular secretion pathway (72), reinforcing the notion that the direct loss of ZnT2 in the MEC impairs the maintenance of a secreting and differentiated epithelium.

Furthermore, we noted abnormal preservation of adipocytes in the mammary gland of ZnT2-null mice, and thus, the inability to deplete adipocytes may have profound implications on developing and/or maintaining a secreting mammary epithelium. Adipocytes secrete numerous factors that can impact mammary gland function, such as leptin and estrogen (73). The persistence of these factors may have adverse consequences on lactation. For example, high levels of leptin suppress milk ejection by inhibiting oxytocin-induced contractions (74, 75). Moreover, prolactin stimulates leptin secretion from mammary adipose, which up-regulates expression of estrogen receptor $\alpha$ and can negatively impact the maintenance of the secreting epithelium through inhibition of Stat signaling in MECs during lactation (76). Because we detected ZnT2 in adipocytes, it is possible that ZnT2-mediated zinc transport plays a role in lactation-induced lipolysis via lipoprotein lipase (55). The inability to clear triglycerides from adipocyte depots may partially underlie the lower level of milk fat observed in ZnT2-null mice. Collectively, our data demonstrate that ZnT2-mediated zinc transport is required for mammary differentiation and the maintenance of a secreting epithelium during lactation.

*Loss of ZnT2 Impairs Milk Secretion*—Consistent with reports in women with mutations in ZnT2, loss of ZnT2 function in ZnT2-null mice reduced milk zinc levels by ~30%. Although milk zinc levels were lower, we do not know if their offspring suffer from zinc deficiency or would survive if we allowed them to age past 10 days. However, in addition to zinc, milk protein, lactose, and fat is significantly lower as well. Thus the impact on offspring survival likely resulted from a general malnutrition. In response to increased prolactin levels at parturition, the differentiated epithelium finely coordinates the synthesis and transport of various milk constituents that are ultimately secreted into the alveolar lumen to provide adequate milk to the developing infant (77). Because milk lipid is a major constituent of mouse milk, the active secretion of lipid droplets from MECs into the alveolar lumen is indicative of the secretory capacity of the mammary gland. Surprisingly, we found a significant accumulation of lipid droplets in the MECs in ZnT2-null mice, suggesting a profound defect in secretory activation (36). Impaired secretion was further verified by reduced milk protein, lactose, and total volume in ZnT2-null mice, resulting in overall suboptimal milk delivery. In addition to the macronutrients described above, milk is a complex biological fluid, and MECs secrete a plethora of bioactive factors, anti-infectious and anti-inflammatory agents, growth factors, and prebiotics, all of which are essential for infant growth and immune development (78). Here, we only report reductions in zinc and macronutrients, but it is probable that dysregulation of numerous cellular secretion pathways suppress the secretion of other micronutrients and non-nutritive factors or may even augment the efflux of unwanted components, thereby producing suboptimal milk and negatively affecting neonatal health.

In summary, our study shows that ZnT2-mediated zinc transport is critical for mammary gland expansion and differentiation and milk secretion during lactation. Collectively, the loss of ZnT2 resulted in mammary gland hypoplasia, the underlying cause of failed lactogenesis II where the mother is unable to produce an adequate milk volume (79). The etiology of breast hypoplasia is unknown, but our observations along with previous studies regarding zinc deficiency and the mammary gland (3–5) suggest that tight regulation of zinc metabolism plays an important role in regulating mammary gland biology.

*Acknowledgments—Images were generated at the Penn State Microscopy and Cytometry Facility, University Park, Pennsylvania and Microscopy Imaging Facility, Section of Research Resources, Penn State Hershey College of Medicine (date of acquisition November 2014). Moreover, we thank the members of the Kelleher laboratory for their constructive comments.*

**References**

1. Neville, M. C. (2009) Introduction: tight junctions and secretory activation in the mammary gland. *J. Mammary Gland Biol. Neoplasia* **14,** 269–270
2. Brisken, C., and Rajaram, R. D. (2006) Alveolar and lactogenic differentiation. *J. Mammary Gland Biol. Neoplasia* **11,** 239–248
3. Bostanci, Z., Mack, R. P., Jr., Lee, S., Soybel, D. I., and Kelleher, S. L. (2014) Paradoxical zinc toxicity and oxidative stress in the mammary gland during marginal dietary zinc deficiency. *Reprod. Toxicol.* 10.1016/j.reprotox.2014.07.076
4. Mutch, P. B., and Hurley, L. S. (1980) Mammary gland function and development: effect of zinc deficiency in rat. *Am. J. Physiol.* **238,** E26–E31
5. Dempsey, C., McCormick, N. H., Croxford, T. P., Seo, Y. A., Grider, A., and Kelleher, S. L. (2012) Marginal maternal zinc deficiency in lactating mice reduces secretory capacity and alters milk composition. *J. Nutr.* **142,** 655–660
6. Eide, D. J. (2006) Zinc transporters and the cellular trafficking of zinc. *Biochim. Biophys. Acta* **1763,** 711–722
7. Palmiter, R. D., and Huang, L. (2004) Efflux and compartmentalization of zinc by members of the SLC30 family of solute carriers. *Pflugers Arch.* **447,** 744–751
8. Kambe, T., Hashimoto, A., and Fujimoto, S. (2014) Current understanding of ZIP and ZnT zinc transporters in human health and diseases. *Cell. Mol. Life Sci.* **71,** 3281–3295
9. Palmiter, R. D., Cole, T. B., and Findley, S. D. (1996) ZnT-2, a mammalian protein that confers resistance to zinc by facilitating vesicular sequestration. *EMBO J.* **15,** 1784–1791
10. Lopez, V., and Kelleher, S. L. (2009) Zinc transporter-2 (ZnT2) variants are localized to distinct subcellular compartments and functionally transport zinc. *Biochem. J.* **422,** 43–52
11. Lasry, I., Golan, Y., Berman, B., Amram, N., Glaser, F., and Assaraf, Y. G. (2014) *In situ* dimerization of multiple wild type and mutant zinc transporters in live cells using bimolecular fluorescence complementation. *J. Biol. Chem.* **289,** 7275–7292
12. Guo, L., Lichten, L. A., Ryu, M. S., Liuzzi, J. P., Wang, F., and Cousins, R. J. (2010) STAT5-glucocorticoid receptor interaction and MTF-1 regulate the expression of ZnT2 (Slc30a2) in pancreatic acinar cells. *Proc. Natl. Acad. Sci. U.S.A.* **107,** 2818–2823
13. Qian, L., Lopez, V., Seo, Y. A., and Kelleher, S. L. (2009) Prolactin regulates ZNT2 expression through the JAK2/STAT5 signaling pathway in mammary cells. *Am. J. Physiol. Cell Physiol.* **297,** C369–C377
14. Seo, Y. A., Lee, S., Hennigar, S. R., and Kelleher, S. L. (2014) Prolactin (PRL)-stimulated ubiquitination of ZnT2 mediates a transient increase in zinc secretion followed by ZnT2 degradation in mammary epithelial cells. *J. Biol. Chem.* **289,** 23653–23661
15. Seo, Y. A., Lopez, V., and Kelleher, S. L. (2011) A histidine-rich motif

mediates mitochondrial localization of ZnT2 to modulate mitochondrial function. *Am. J. Physiol. Cell Physiol.* **300,** C1479–C1489
16. Chowanadisai, W., Lönnerdal, B., and Kelleher, S. L. (2006) Identification of a mutation in SLC30A2 (ZnT-2) in women with low milk zinc concentration that results in transient neonatal zinc deficiency. *J. Biol. Chem.* **281,** 39699–39707
17. Itsumura, N., Inamo, Y., Okazaki, F., Teranishi, F., Narita, H., Kambe, T., and Kodama, H. (2013) Compound heterozygous mutations in SLC30A2/ZnT2 results in low milk zinc concentrations: a novel mechanism for zinc deficiency in a breast-fed infant. *PLoS ONE* **8,** e64045
18. Miletta, M. C., Bieri, A., Kernland, K., Schöni, M. H., Petkovic, V., Flück, C. E., Eblé, A., and Mullis, P. E. (2013) Transient neonatal zinc deficiency caused by a heterozygous G87R mutation in the zinc transporter ZnT-2 (SLC30A2) gene in the mother highlighting the importance of $Zn^{2+}$ for normal growth and development. *Int. J. Endocrinol.* **2013,** 259189
19. Dórea, J. G. (2002) Zinc deficiency in nursing infants. *J. Am. Coll. Nutr.* **21,** 84–87
20. Piela, Z., Szuber, M., Mach, B., and Janniger, C. K. (1998) Zinc deficiency in exclusively breast-fed infants. *Cutis* **61,** 197–200
21. Chua, A. C., Hodson, L. J., Moldenhauer, L. M., Robertson, S. A., and Ingman, W. V. (2010) Dual roles for macrophages in ovarian cycle-associated development and remodelling of the mammary gland epithelium. *Development* **137,** 4229–4238
22. Bostanci, Z., Alam, S., Soybel, D. I., and Kelleher, S. L. (2014) Prolactin receptor attenuation induces zinc pool redistribution through ZnT2 and decreases invasion in MDA-MB-453 breast cancer cells. *Exp. Cell Res.* **321,** 190–200
23. Clegg, M. S., Keen, C. L., Lönnerdal, B., and Hurley, L. S. (1981) Influence of ashing techniques on the analysis of trace elements in animal tissue: I. Wet ashing. *Biol. Trace Elem. Res.* **3,** 107–115
24. McCormick, N. H., and Kelleher, S. L. (2012) ZnT4 provides zinc to zinc-dependent proteins in the trans-Golgi network critical for cell function and $Zn^{2+}$ export in mammary epithelial cells. *Am. J. Physiol. Cell Physiol.* **303,** C291–C297
25. Hanania, R., Sun, H. S., Xu, K., Pustylnik, S., Jeganathan, S., and Harrison, R. E. (2012) Classically activated macrophages use stable microtubules for matrix metalloproteinase-9 (MMP-9) secretion. *J. Biol. Chem.* **287,** 8468–8483
26. Sbai, O., Ferhat, L., Bernard, A., Gueye, Y., Ould-Yahoui, A., Thiolloy, S., Charrat, E., Charton, G., Tremblay, E., Risso, J. J., Chauvin, J. P., Arsanto, J. P., Rivera, S., and Khrestchatisky, M. (2008) Vesicular trafficking and secretion of matrix metalloproteinases-2 and -9 and tissue inhibitor of metalloproteinases-1 in neuronal cells. *Mol. Cell. Neurosci.* **39,** 549–568
27. Taraboletti, G., D'Ascenzo, S., Borsotti, P., Giavazzi, R., Pavan, A., and Dolo, V. (2002) Shedding of the matrix metalloproteinases MMP-2, MMP-9, and MT1-MMP as membrane vesicle-associated components by endothelial cells. *Am. J. Pathol.* **160,** 673–680
28. Kelleher, S. L., McCormick, N. H., Velasquez, V., and Lopez, V. (2011) Zinc in specialized secretory tissues: roles in the pancreas, prostate, and mammary gland. *Adv. Nutr.* **2,** 101–111
29. Fata, J. E., Leco, K. J., Moorehead, R. A., Martin, D. C., and Khokha, R. (1999) Timp-1 is important for epithelial proliferation and branching morphogenesis during mouse mammary development. *Dev. Biol.* **211,** 238–254
30. Gouon-Evans, V., Rothenberg, M. E., and Pollard, J. W. (2000) Postnatal mammary gland development requires macrophages and eosinophils. *Development* **127,** 2269–2282
31. Kelleher, S. L., Velasquez, V., Croxford, T. P., McCormick, N. H., Lopez, V., and MacDavid, J. (2012) Mapping the zinc-transporting system in mammary cells: molecular analysis reveals a phenotype-dependent zinc-transporting network during lactation. *J. Cell Physiol.* **227,** 1761–1770
32. Kelleher, S. L., and Lönnerdal, B. (2003) zinc transporter levels and localization change throughout lactation in rat mammary gland and are regulated by $Zn^{2+}$ in mammary cells. *J. Nutr.* **133,** 3378–3385
33. McCormick, N., Velasquez, V., Finney, L., Vogt, S., and Kelleher, S. L. (2010) X-ray fluorescence microscopy reveals accumulation and secretion of discrete intracellular zinc pools in the lactating mouse mammary gland. *PLoS ONE* **5,** e11078
34. Lopez, V., Foolad, F., and Kelleher, S. L. (2011) ZnT2-overexpression represses the cytotoxic effects of zinc hyper-accumulation in malignant metallothionein-null T47D breast tumor cells. *Cancer Lett.* **304,** 41–51
35. Grigor, M. R., Poczwa, Z., and Arthur, P. G. (1986) Milk lipid synthesis and secretion during milk stasis in the rat. *J. Nutr.* **116,** 1789–1797
36. Zhang, L., Reidy, S. P., Bogachev, O., Hall, B. K., Majdalawieh, A., and Ro, H. S. (2011) Lactation defect with impaired secretory activation in AEBP1-null mice. *PLoS ONE* **6,** e27795
37. Bachiller, P. R., Cornog, K. H., Kato, R., Buys, E. S., and Roberts, J. D., Jr. (2013) Soluble guanylate cyclase modulates alveolarization in the newborn lung. *Am. J. Physiol. Lung Cell Mol. Physiol.* **305,** L569–L581
38. Watson, C. J. (2006) Involution: apoptosis and tissue remodelling that convert the mammary gland from milk factory to a quiescent organ. *Breast Cancer Res.* **8,** 203
39. Colitti, M., and Farinacci, M. (2009) Cell turnover and gene activities in sheep mammary glands prior to lambing to involution. *Tissue Cell* **41,** 326–333
40. Chapman, R. S., Lourenco, P., Tonner, E., Flint, D., Selbert, S., Takeda, K., Akira, S., Clarke, A. R., and Watson, C. J. (2000) The role of Stat3 in apoptosis and mammary gland involution: conditional deletion of Stat3. *Adv. Exp. Med. Biol.* **480,** 129–138
41. Cui, Y., Riedlinger, G., Miyoshi, K., Tang, W., Li, C., Deng, C. X., Robinson, G. W., and Hennighausen, L. (2004) Inactivation of Stat5 in mouse mammary epithelium during pregnancy reveals distinct functions in cell proliferation, survival, and differentiation. *Mol. Cell. Biol.* **24,** 8037–8047
42. Iavnilovitch, E., Groner, B., and Barash, I. (2002) Overexpression and forced activation of stat5 in mammary gland of transgenic mice promotes cellular proliferation, enhances differentiation, and delays postlactational apoptosis. *Mol. Cancer Res.* **1,** 32–47
43. Hennighausen, L., and Robinson, G. W. (2005) Information networks in the mammary gland. *Nat. Rev. Mol. Cell Biol.* **6,** 715–725
44. McManaman, J. L., and Neville, M. C. (2003) Mammary physiology and milk secretion. *Adv. Drug. Deliv. Rev.* **55,** 629–641
45. Miyoshi, K., Shillingford, J. M., Smith, G. H., Grimm, S. L., Wagner, K. U., Oka, T., Rosen, J. M., Robinson, G. W., and Hennighausen, L. (2001) Signal transducer and activator of transcription 5 (Stat5) controls the proliferation and differentiation of mammary alveolar epithelium. *J. Cell Biol.* **155,** 531–542
46. Michalczyk, A. A., Allen, J., Blomeley, R. C., and Ackland, M. L. (2002) Constitutive expression of hZnT4 zinc transporter in human breast epithelial cells. *Biochem. J.* **364,** 105–113
47. Kambe, T., Yamaguchi-Iwai, Y., Sasaki, R., and Nagao, M. (2004) Overview of mammalian zinc transporters. *Cell. Mol. Life Sci.* **61,** 49–68
48. Campbell, J. J., and Watson, C. J. (2009) Three-dimensional culture models of mammary gland. *Organogenesis* **5,** 43–49
49. Wiseman, B. S., Sternlicht, M. D., Lund, L. R., Alexander, C. M., Mott, J., Bissell, M. J., Soloway, P., Itohara, S., and Werb, Z. (2003) Site-specific inductive and inhibitory activities of MMP-2 and MMP-3 orchestrate mammary gland branching morphogenesis. *J. Cell Biol.* **162,** 1123–1133
50. Ke, Z., Lin, H., Fan, Z., Cai, T. Q., Kaplan, R. A., Ma, C., Bower, K. A., Shi, X., and Luo, J. (2006) MMP-2 mediates ethanol-induced invasion of mammary epithelial cells over-expressing ErbB2. *Int. J. Cancer* **119,** 8–16
51. Khokha, R., and Werb, Z. (2011) Mammary gland reprogramming: metalloproteinases couple form with function. *Cold Spring Harb. Perspect. Biol.* **3,** a004333
52. Humphreys, R. C., Krajewska, M., Krnacik, S., Jaeger, R., Weiher, H., Krajewski, S., Reed, J. C., and Rosen, J. M. (1996) Apoptosis in the terminal endbud of the murine mammary gland: a mechanism of ductal morphogenesis. *Development* **122,** 4013–4022
53. Jiang, D., Sullivan, P. G., Sensi, S. L., Steward, O., and Weiss, J. H. (2001) Zn(2+) induces permeability transition pore opening and release of pro-apoptotic peptides from neuronal mitochondria. *J. Biol. Chem.* **276,** 47524–47529
54. Wiseman, B. S., and Werb, Z. (2002) Stromal effects on mammary gland development and breast cancer. *Science* **296,** 1046–1049
55. Hovey, R. C., and Aimo, L. (2010) Diverse and active roles for adipocytes during mammary gland growth and function. *J. Mammary Gland Biol. Neoplasia* **15,** 279–290

56. Landskroner-Eiger, S., Park, J., Israel, D., Pollard, J. W., and Scherer, P. E. (2010) Morphogenesis of the developing mammary gland: stage-dependent impact of adipocytes. *Dev. Biol.* **344,** 968–978
57. Coulston, L., and Dandona, P. (1980) Insulin-like effect of zinc on adipocytes. *Diabetes* **29,** 665–667
58. Shisheva, A., Gefel, D., and Shechter, Y. (1992) Insulinlike effects of zinc ion *in vitro* and *in vivo*. Preferential effects on desensitized adipocytes and induction of normoglycemia in streptozocin-induced rats. *Diabetes* **41,** 982–988
59. Roberts, R., Hodson, L., Dennis, A. L., Neville, M. J., Humphreys, S. M., Harnden, K. E., Micklem, K. J., and Frayn, K. N. (2009) Markers of *de novo* lipogenesis in adipose tissue: associations with small adipocytes and insulin sensitivity in humans. *Diabetologia* **52,** 882–890
60. Kamikawa, A., Ichii, O., Yamaji, D., Imao, T., Suzuki, C., Okamatsu-Ogura, Y., Terao, A., Kon, Y., and Kimura, K. (2009) Diet-induced obesity disrupts ductal development in the mammary glands of nonpregnant mice. *Dev. Dyn.* **238,** 1092–1099
61. Trujillo, M. E., and Scherer, P. E. (2006) Adipose tissue-derived factors: impact on health and disease. *Endocr. Rev.* **27,** 762–778
62. Reed, J. R., and Schwertfeger, K. L. (2010) Immune cell location and function during post-natal mammary gland development. *J. Mammary Gland Biol. Neoplasia* **15,** 329–339
63. Fleming, J. M., Miller, T. C., Kidacki, M., Ginsburg, E., Stuelten, C. H., Stewart, D. A., Troester, M. A., and Vonderhaar, B. K. (2012) Paracrine interactions between primary human macrophages and human fibroblasts enhance murine mammary gland humanization *in vivo*. *Breast Cancer Res.* **14,** R97
64. O'Brien, J., Martinson, H., Durand-Rougely, C., and Schedin, P. (2012) Macrophages are crucial for epithelial cell death and adipocyte repopulation during mammary gland involution. *Development* **139,** 269–275
65. Ucar, A., Vafaizadeh, V., Jarry, H., Fiedler, J., Klemmt, P. A., Thum, T., Groner, B., and Chowdhury, K. (2010) miR-212 and miR-132 are required for epithelial stromal interactions necessary for mouse mammary gland development. *Nat. Genet.* **42,** 1101–1108
66. Shankar, A. H., and Prasad, A. S. (1998) Zinc and immune function: the biological basis of altered resistance to infection. *Am. J. Clin. Nutr.* **68,** 447S–463S
67. Bhardwaj, P., Du, B., Zhou, X. K., Sue, E., Harbus, M. D., Falcone, D. J., Giri, D., Hudis, C. A., Kopelovich, L., Subbaramaiah, K., and Dannenberg, A. J. (2013) Caloric restriction reverses obesity-induced mammary gland inflammation in mice. *Cancer Prev. Res. (Phila)* **6,** 282–289
68. Schwertfeger, K. L., Rosen, J. M., and Cohen, D. A. (2006) Mammary gland macrophages: pleiotropic functions in mammary development. *J. Mammary Gland Biol. Neoplasia* **11,** 229–238
69. Watson, C. J., and Burdon, T. G. (1996) Prolactin signal transduction mechanisms in the mammary gland: the role of the Jak/Stat pathway. *Rev. Reprod.* **1,** 1–5
70. Chen, C. C., Stairs, D. B., Boxer, R. B., Belka, G. K., Horseman, N. D., Alvarez, J. V., and Chodosh, L. A. (2012) Autocrine prolactin induced by the Pten-Akt pathway is required for lactation initiation and provides a direct link between the Akt and Stat5 pathways. *Genes Dev.* **26,** 2154–2168
71. Chen, Y., Wen, R., Yang, S., Schuman, J., Zhang, E. E., Yi, T., Feng, G. S., and Wang, D. (2003) Identification of Shp-2 as a Stat5A phosphatase. *J. Biol. Chem.* **278,** 16520–16527
72. Stelwagen, K., McFadden, H. A., and Demmer, J. (1999) Prolactin, alone or in combination with glucocorticoids, enhances tight junction formation and expression of the tight junction protein occludin in mammary cells. *Mol. Cell. Endocrinol.* **156,** 55–61
73. Feuermann, Y., Mabjeesh, S. J., and Shamay, A. (2009) Mammary fat can adjust prolactin effect on mammary epithelial cells via leptin and estrogen. *Int. J. Endocrinol.* **2009,** 427260
74. Jevitt, C., Hernandez, I., and Groër, M. (2007) Lactation complicated by overweight and obesity: supporting the mother and newborn. *J. Midwifery Womens Health* **52,** 606–613
75. Moynihan, A. T., Hehir, M. P., Glavey, S. V., Smith, T. J., and Morrison, J. J. (2006) Inhibitory effect of leptin on human uterine contractility *in vitro*. *Am. J. Obstet. Gynecol.* **195,** 504–509
76. Thorn, S. R., Giesy, S. L., Myers, M. G., Jr., and Boisclair, Y. R. (2010) Mammary ductal growth is impaired in mice lacking leptin-dependent signal transducer and activator of transcription 3 signaling. *Endocrinology* **151,** 3985–3995
77. Neville, M. C., and Mather, I. H. (2007) Introduction: secretory activation: from the past to the future. *J. Mammary Gland Biol. Neoplasia* **12,** 205–210
78. Ballard, O., and Morrow, A. L. (2013) Human milk composition: nutrients and bioactive factors. *Pediatr. Clin. North Am.* **60,** 49–74
79. Arbour, M. W., and Kessler, J. L. (2013) Mammary hypoplasia: not every breast can produce sufficient milk. *J. Midwifery Womens Health* **58,** 457–461